energies

MDPI

Article

Off-Design Performances of an Organic Rankine Cycle for Waste Heat Recovery from Gas Turbines

Carlo Carcasci *, Lapo Cheli, Pietro Lubello and Lorenzo Winchler

DIEF—Department of Industrial Engineering, University of Florence Via Santa Marta, 3, 50139 Florence, Italy; lapo.cheli@unifi.it (L.C.); pietro.lubello@unifi.it (P.L.); lorenzo.winchler@htc.de.unifi.it (L.W.)

* Correspondence: carlo.carcasci@unifi.it

Received: 24 January 2020; Accepted: 26 February 2020; Published: 2 March 2020

Abstract: This paper presents an off-design analysis of a gas turbine Organic Rankine Cycle (ORC) combined cycle. Combustion turbine performances are significantly affected by fluctuations in ambient conditions, leading to relevant variations in the exhaust gases' mass flow rate and temperature. The effects of the variation of ambient air temperature have been considered in the simulation of the topper cycle and of the condenser in the bottomer one. Analyses have been performed for different working fluids (toluene, benzene and cyclopentane) and control systems have been introduced on critical parameters, such as oil temperature and air mass flow rate at the condenser fan. Results have highlighted similar power outputs for cycles based on benzene and toluene, while differences as high as 34% have been found for cyclopentane. The power output trend with ambient temperature has been found to be influenced by slope discontinuities in gas turbine exhaust mass flow rate and temperature and by the upper limit imposed on the air mass flow rate at the condenser as well, suggesting the importance of a correct sizing of the component in the design phase. Overall, benzene-based cycle power output has been found to vary between 4518 kW and 3346 kW in the ambient air temperature range considered.

Keywords: ORC integration technologies; advanced thermodynamic cycles; decentralised energy systems; benzene; toluene; cyclopentane

1. Introduction

In recent years, the accelerated consumption of fossil fuels caused many serious environmental problems, such as global warming, depletion of the ozone layer and atmospheric pollution. A statistic survey from Hung [1] demonstrated that more than 50% of waste heat produced by industries is at low temperatures and therefore is difficult to recover with conventional systems based on Rankine steam cycle.

Organic Rankine Cycle (ORC) power plants have proved to be an attractive solution for the conversion of low/medium grade heat into electricity. Furthermore, this kind of cycle allows the usage of clean energy sources, such as solar radiation [2], geothermal water/steam [3,4], biomass [5] and waste combustion. ORC works on organic fluids, which usually have higher molecular weight and lower evaporation points with respect to water: this permits the increase of the efficiency when working below 400–500 °C. Dry fluids are preferred because of the positive slope of their saturation vapour curve that prevents liquid formation during expansion [6]. This choice is also based on environmental impact: several studies on the fluid's polluting properties can be found in literature, as in the work of Chen [7]. ORC power plants tend to have numerous advantages, such as reliability, quiet operation, long life and compact size [8].

Many studies can be found in the literature, in particular on thermodynamic analysis with several fluids and design optimisation: it has been observed that to avoid the formation of wet fraction

expansion when the cycle is not overheated, the evaporation pressure must not exceed the pressure characterised by the maximum saturation specific entropy [9]. The most significant parameters influencing cycle performances are pinch point temperature difference, fluid flow and inlet evaporator diathermic oil temperature [10–14]. It should be noted that the expander, condenser and evaporator generate the greater part of the exergetic losses, which tend to increment with increasing expander inlet temperature and gas temperature [15,16].

Several papers have focused on combined cycles employing gas turbine as topper cycle and alternative solutions to the traditional steam-water Rankine cycle for the bottoming one. Chacartegui [17] proposed ORC as an alternative bottoming cycle for a combined cycle power plant, while Del Turco [18] proposed the so-called *ORegen cycle*. Carcasci [19] studied the ORC bottoming cycle at design conditions for different working fluids (benzene, toluene and cyclopentane), showing the best efficiency settings by varying fluid evaporation pressure and oil temperature, with a GE10 gas turbine [20]. More recent papers have studied the behaviour of Organic Rankine Cycle in off-design conditions, e.g., Quoilin [21] have studied a regulation dynamic model for transitional state and off-design. They proposed three different strategies for expander and pump control systems and have demonstrated that the most effective one is the evaporation temperature optimisation according to the working conditions. Song [22] analysed the behaviour of an ORC system using a parametric analysis and a one-dimensional analysis method for the aerodynamic model of the turbine, working both under design and off-design conditions; the inlet temperatures of the heat source and the cooling water were found to have a significant influence on the system performance. Cao [23] presents a comparative analysis on the off-design performance of a gas turbine and organic Rankine cycle (GT-ORC) combined cycle under different operation approaches; the GT-ORC cycle efficiency was maximised with a sliding pressure operation method in order to reduce the influence of ambient temperature on the overall efficiency.

Another dynamic control model was demonstrated by Wei [24], who obtained an accuracy of 4% without presenting numerical inaccuracies due to the oscillation phenomena. Manente [4] analyzed an ORC for geothermal heat recovery. The key elements of the dynamic model were two tanks, one at high and one at low pressure, which made the two main flows independent respectively to the expander and to the pump. By varying the ambient and geothermal fluid temperature, they have optimised the performance by changing the pump's revolutions per minute, turbine's capacity factor and condenser's refrigerant mass flow rate. The authors have identified a limit in the optimisation of the cycle: the geothermal fluid reinjection temperature should not be less than 70 °C. Sauret [25] performed a three-dimensional off-design numerical analysis of an ORC. First, they identified R143a as the best high density fluid to optimise the turbine's outlet power, then they analysed the radial-inflow turbine operation in several part-load conditions. Fu [26] investigated the cycle performance by varying the heat source temperature: an increment of this parameter generates an increase in net power and heat transfer capacity. Ibarra [27] computed the Organic Rankine Cycle performance at several imposed power outputs, using R245fa and SES36 fluids; by varying expansion speed and working pressure they obtained the off-design maximum efficiency.

Bamgbopa [28] employed an unsteady model to analyse the efficiency of a solar ORC while comparing different working fluid mass flow rates, heat source temperatures and heat source mass flow rates. De Escalona [29], in order to identify the best part-load control strategy of a gas turbine combined with ORC, has maintained the efficiency of the bottomer cycle at the design value by imposing a constant evaporating pressure. The topper cycle efficiency decreases with the load. When this happens the heat supplied to the ORC increases, resulting in a higher power output and better overall performances. Lecompte [30] developed a thermo-economic optimisation method minimising the investment specific cost at partial loads Specific Investment Cost Part Load (SICPL); SICPL is a polynomial expression depending on ambient temperature and supplied thermal power. The authors proved that investment specific costs increase from design conditions to variable thermodynamic ones. Calise [31] proposed another thermo-economic optimisation model, based on investment costs

minimisation. In off-design conditions, they noted an increase in the cycle's power output in the presence of a fluid mass flow rate decrease. Finally, Quoilin [32] demonstrated that better performances can be obtained for evaporation temperatures significantly lower than the heat source one, while for higher values (ensuring higher pressures and densities) the economic optimum is obtained due to the smaller size of the heat exchanger.

The novelty of the presented work is the study of the off-design performances of an ORC with the inclusion of its control system; moreover, the ORC is fed by waste heat recovered from a gas turbine exhaust, employing a similar cycle to the one described by Carcasci [33]. The analysis has been conducted for three different working fluids (benzene, toluene and cyclopentane) and has been performed varying the ambient air temperature while monitoring the cycle's characteristic parameters. Related trends are identified and control limits imposed to avoid exceeding in working conditions the imposed boundaries for critical parameters.

2. Materials and Methods

2.1. Working Fluid

The considered working fluids are benzene, toluene and cyclopentane. When a working fluid for ORC application is chosen, several criteria need to be considered: environmental sustainability, safety, thermal stability and critical temperature. The employed fluids meet most of the criteria listed, indeed ORC cycles based on such fluids are widely analysed in the literature [17,18]. The three fluids are dry and belong to the hydrocarbons family: the first two are aromatic and the third is a cycloalkane. Typically, dry fluids are preferred, since superheating is not necessary in order to avoid condensation during vapor expansion. To simulate the fluids behaviour, a NIST software was employed (NIST4 in the specific application).

Critical temperatures reported in Table 1 are high enough to guarantee a wide saturation curve and great chemical stability at the analysed temperatures. Table 1 shows also high molar masses (and densities), which allow a high specific heat absorption for each fluid, thus reducing the required mass flow rate. This enables the reduction of power consumption, pump size and the required surface for the heat exchangers, therefore decreasing the overall plant size and its cost. Moreover, smaller mass flow rates imply reduced environmental impact.

Table 1. Thermodynamic properties of selected working fluids.

Working Fluid	T_{cr} (°C)	P_{cr} (bar)	M_m (g/mol)	$P_{s,max}$ (bar)
Toluene	318.6	41.1	92.14	36.0
Benzene	288.8	48.9	78.10	37.5
Cyclopentane	238.6	44.3	70.13	34.7

The often used pollution indices are the Global Warming Potential (GWP) and Ozone Depletion Potential (ODP). Hydrocarbons have low GWP (between 3 and 24 units in the case of gas methane) and zero ODP, since they do not contain chlorine or bromine atoms. Another positive aspect is the low electrical conductivity, which allows the fluids to be used as lubricant for the turbine's bearings and as coolant for the generator. On the other hand, some of these fluids have negative effects on human health: at ambient conditions, benzene is volatile, colourless, highly flammable, irritant and carcinogenic on long-term exposure; toluene is irritant as well, but less volatile and toxic than benzene; cyclopentane is the most flammable of the three fluids, with a visibly lower auto ignition temperature of 380 °C but a reduced adverse effect on human health, as demonstrated by the higher Threshold Limit Value (TLV). Saturation temperature value, as determined by *NIST4* library, has been plotted as a function of pressure for each organic fluid and is reported in Figure 1: toluene shows the higher saturation temperature regardless of the pressure considered, while cyclopentane shows the lowest.

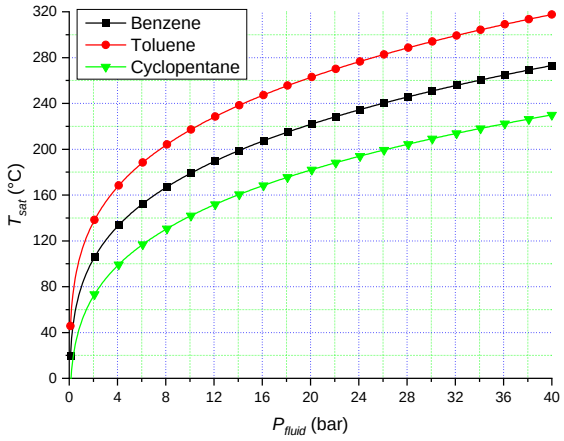

Figure 1. Saturation temperature vs. pressure for each organic fluid.

2.2. Power Plant Layout

The examined plant is based on the traditional subcritical Rankine cycle, combined with a gas turbine topping cycle. Figure 2 shows the power plant layout of the ORC bottoming cycle [19].

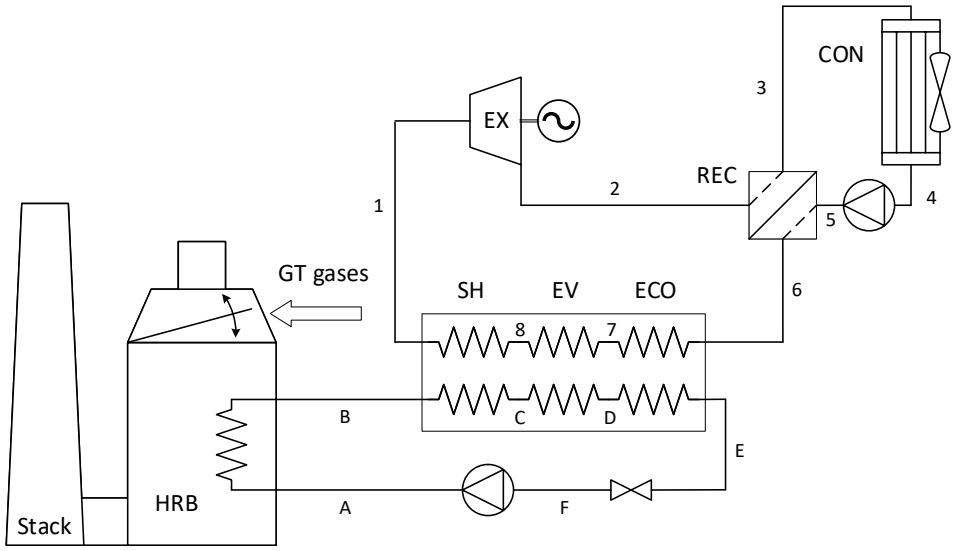

Figure 2. Organic Rankine Cycle (ORC) power plant layout. Points 1–8: organic fluid cycle, points A–F: diathermic oil cycle

The gas turbine is the GE10-1 from General Electric–Nuovo Pignone; it is a heavy-duty single-shaft gas turbine used for power generation applications [20]. Table 2 lists the main specifications of the considered gas turbine. For safety reasons, the recovery cycle is designed for a heat transfer made by an intermediate diathermic oil circuit placed between the hot gas turbine exhaust flow and the organic fluid loop.

Table 2. GE10 single shaft gas turbine main specification [20].

W_{GT} (kW)	η_{GT} (%)	m_{EXH} (kg/s)	T_{EXH} (°C)
11,250	31.4	47.5	482.0

The cycle has only one pressure level and, in order to increase the system efficiency, a recuperative heat exchanger (REC) has been introduced. The hot exhaust gas mass flow (first cycle) heats the diathermic oil (second cycle, points A to F) in the heat recovery boiler (HRB), the hot oil passes then through the heat recovery steam generator (points B-E), composed by economizer (ECO), evaporator (EV) and superheater (SH). A third separated cycle is the organic fluid loop (points 1–8). After leaving the HRSG, the superheated fluid enters the turbo-expander (EX). The exhaust organic fluid exchanges then heats in the recuperator (REC), where the condensed fluid is heated. Finally, the organic fluid is cooled in a condenser (CON) and pressurised in the extraction pump. The condenser is of an air-cooled type, as the application in water-scarce areas has been considered.

2.3. Off-Design Analysis

When the plant works in off-design conditions, the temperature difference between the hot and cold fluid cannot be imposed, while the geometry (heat exchange surfaces) is the same obtained in the design phase. The surface is determined in the design condition by imposing the temperature difference, energy balances and mass flow rates. Through the logarithmic mean temperature difference the overall heat transfer coefficient UA value in design condition can be determined:

$$UA_{des} = \frac{Q}{\Delta T_{ml}} \tag{1}$$

In the Heat Recovery Boiler (HRB), temperature and mass flow rate of gas turbine's exhaust gas are imposed (m_{exh}, T_{exh}; see Table 2 and Figure 3) and maximum oil temperature is limited by the oil properties: $T_B = T_{oil,max} = 380$ °C.

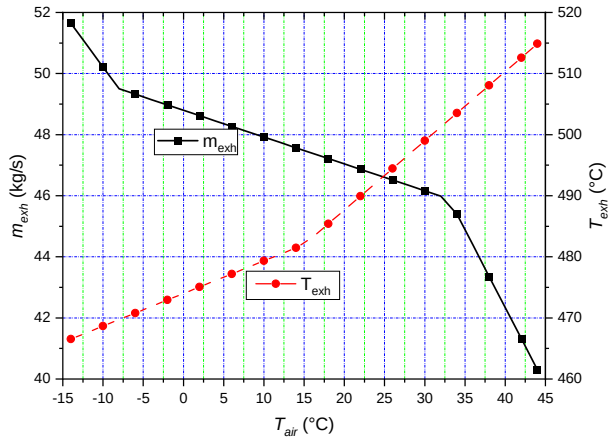

Figure 3. Mass flow rate and temperature exhaust from GE10 gas turbine, varying ambient temperature.

Contrary to design analysis, pinch point cannot be imposed, but the UA_{HRB} in gas-oil heat recovery boiler is imposed instead, and by using the energy balance, stack temperature of the hot gas stream can be determined. This value must be higher than stack temperature limit—$T_{st,lim} =$ 90 °C—to avoid the occurrence of corrosion phenomena. Moreover, the oil mass flow rate (m_{oil}) can be determined: the control system sets the maximum oil temperature that will be obtained by varying the oil valve position and pump settings, thus allowing the oil mass flow rate to vary consequently.

On the other side of the plant, considering that ambient conditions are known (even though different from the design case), employing the energy balance and the overall heat transfer coefficient of the condenser (UA_{con}), the outlet air temperature ($T_{air,out}$) can be determined. This can be done by dividing the condenser in two sections, one for the condensation and one for the vapour cooling, and by imposing the organic fluid saturation pressure ($P_4 = P_{con}$). Furthermore, the air mass flow rate of the fan condenser (m_{air}) is determined using the energy balance in the condenser. The power absorbed by the fan (W_{fan}) can be determined as well:

$$W_{fan} = m_{con,air} \frac{\Delta P_{con,air}}{\rho_{air}} \tag{2}$$

In practice, the control system varies the fan speed to obtain the imposed condenser pressure (maintained constant), even though the fan and its electric motor have performance limits. The reduced mass flow rate in the expander and the exhaust pressure (from the condenser balance) can be determined but they depend on the expander characteristic. There are two different ways to proceed:

- Working with a fixed expander nondimensional flow, so that the inlet pressure can vary (the inlet pressure is set by the expander characteristic and the expander is often chocked, resulting in a constant reduced mass flow rate, compared to the design condition [9])
- Working with a control system: the analysed cycle has only one level of evaporating pressure with an internal heat exchanger, the recuperator (REC), to increase the system efficiency (valve) at the inlet of the expander that allows for the setting of the pressure

In any case, it is possible to start imposing the maximum fluid pressure and, together with the UA in the evaporator (EV) and the energy balance, the organic fluid mass flow rate can be calculated. The exhaust condition of the organic fluid from the $HRSG$ is considered to be saturated steam at maximum pressure. If the superheater (SH) is present, another energy balance is necessary and its UA_{SH} to obtain the exhaust organic fluid temperature. If the expander is equipped with an inlet pressure control system, it adjusts the expander to the inlet flow conditions. If the inlet pressure control system is not present, the mass flow rate and pressure at the inlet of the expander must match its characteristic curve. Supposing that the expander is chocked, the nondimensional flow is constant (and has been determined in design condition). The inlet pressure cannot be imposed and has to be obtained from the following equation:

$$\frac{m_{fl,off} \cdot \sqrt{T_{1,off}}}{P_{1,off}} = \frac{m_{fl} \cdot \sqrt{T_1}}{P_1} = constant \tag{3}$$

Thus, an iterative calculation is necessary between the evaporator (superheater, if present) and the expander, indeed the organic fluid mass flow rate and the maximum pressure are determined by matching these components. The isentropic efficiency depends on the expander operating conditions [31]. Once computed, it allows the organic fluid exhaust conditions to be obtained. Applying the energy balance and heat transfer equations at the recuperator (REC), the organic fluid conditions at the inlet of the condenser (CON) and economizer (ECO) can be determined. A new value for the return oil temperature and for the organic fluid inlet condition at the evaporator are computed, hence closing the oil and organic fluid loops.

The global electrical power output can be determined:

$$W_{el} = m_{fl} \cdot (L_{ex} - L_{pump,fl} - L_{pump,oil}) - W_{fan} \tag{4}$$

A mass balance between the design and off-design cases has to be introduced in order to verify the continuity between the mass flow rates. If the balance is not verified, a tank has to be considered to compensate the mass flow rate fluctuations in the system. In the present study, the mass conservation

is not considered due to the introduction of a tank. The fluid-dependent design conditions (Table 3) considered have been chosen for having the best performance for each fluid (as shown by previous studies like [9,19] at ISO conditions). Table 4 lists all the physical quantities that have been imposed in the design phase independently from the fluid considered. Once the thermodynamic computation of the cycle has been performed, parameters such as the logarithmic mean temperature difference (ΔT_{ml}), UA for each heat exchanger, dimensionless mass flow rate and expander pressure ratio can be determined.

Table 3. ORC power plant data in design conditions—parameters depending on working fluid.

Working Fluid	P_{des} (bar)	$m_{fl,des}$ (kg/s)	$m_{oil,des}$ (kg/s)	$W_{wl,des}$ (kW)
Toluene	36.0	30.52	30.04	4389.9
Benzene	37.5	33.15	29.56	4504.5
Cyclopentane	44.0	22.71	32.95	3652.7

Table 4. ORC power plant data in design conditions—parameters not depending on working fluid.

Parameter	Value	Parameter	Value
$T_{oil,max}$	380.0 °C	$\Delta T_{pp,CON}$	20.0 °C
$\Delta T_{pp,HRSG}$	8.0 °C	$\Delta T_{air,CON}$	20.0 °C
$\Delta T_{app,HRSG}$	30.0 °C	$\Delta T_{pp,REC}$	15.0 °C
$\Delta T_{sub,HRSG}$	15.0 °C	η_{HRB}	0.98
$\Delta T_{pp,HRB}$	10.0 °C	η_{EX}	0.85
$\Delta T_{sub,HRB}$	8.0 °C	η_{pump}	0.70

The authors developed an in-house code that is able to perform thermodynamic simulations of the proposed power plant. The code has been developed in ANSI Standard of the FORTRAN90 programming language and the elementary energy balances have been validated through the comparison with a commercial code.

2.4. Heat Exchanger HTC in Off-Design Conditions

In the previous paragraph, the UA in each section of heat recovery boiler and heat exchanger has been imposed. This value is calculated in design phase, but it changes in off-design conditions. In the present study, a simplified method to determine this value is proposed. The overall heat transfer coefficient is composed of three different parts, respectively addressing internal convection, external convection and conduction through the metal:

$$\frac{1}{U} = \frac{1}{U_{int}} + \frac{1}{k/s} + \frac{1}{U_{ext}} \tag{5}$$

Each thermal factor can be expressed as a fraction of the global thermal resistance

$$\begin{aligned} f_{int} &= \frac{R_{int}}{R} = \frac{U}{U_{int}} \\ f_{cond} &= \frac{R_{cond}}{R} = \frac{U}{k/s} \\ f_{ext} &= \frac{R_{ext}}{R} = \frac{U}{U_{ext}} \end{aligned} \tag{6}$$

to obtain

$$f_{int} + f_{cond} + f_{ext} = 1 \tag{7}$$

From prior knowledge of the mechanism of heat exchange characterising the considered heat exchanger, it is possible to determine the values of the addends f and, as a consequence, of the global

heat transfer coefficient in design conditions. Typically, f_{cond} lies between 0.02 and 0.05, while f_{int} and f_{ext} tend to be between 0.30 and 0.60, depending if describing a component with higher external (e.g., superheater) or internal convection (e.g., economizer). In off-design analysis, the heat transfer coefficient is a function of the mass flow rate and fluid properties. Usually, a correlation for the heat transfer coefficient can be defined through Nusselt and Reynolds numbers [8]. Typical values for the exponent a are between 0.5 and 0.8.

$$Nu = C \cdot Re^a \rightarrow U \propto m^a \rightarrow \frac{U_{off}}{U_{des}} \propto \left(\frac{m_{off}}{m_{des}}\right)^a \tag{8}$$

Thus, with the off-design mass flow rate, the heat transfer coefficient of each contribution can be determined and, by considering the conduction thermal resistance of the metal (k/s) to be constant, the overall heat transfer coefficient can be calculated through Equation (5).

2.5. Critical Conditions and Valve Settings

Control devices are necessary to allow the power plant control in off-design conditions. Indeed, some critical conditions must be avoided:

- Stack temperature must not descend below a certain limit temperature to avoid corrosion phenomena: $T_{st} \geq T_{st,lim} = 90\ ^\circ C$;
- The oil mass flow rate cannot exceed an upper limit (generally referred to the design value): $\alpha_{oil,low} \leq m_{oil}/m_{oil,des} \leq \alpha_{oil,up}$;
- The condenser air mass flow rate cannot exceed a lower and upper limit (generally referred to the design value and depending on fan size, increasing this value raises the fan cost [18]): $m_{con,air}/m_{con,air,des} \leq \alpha_{air,up}$;
- In the recuperator (REC), the organic fluid in the hot section must not reach saturation at outlet (otherwise, transportation of a two-phase fluid into a tube can be challenging);
- In the economizer (ECO), the fluid at the outlet must be subcooled in order to avoid any presence of vapour fraction into the economizer.

Hence, valves must be introduced throughout the power plant to enforce these bounds. A valve can be described by its flow coefficient:

$$CV = \frac{m}{\rho} \cdot \sqrt{\frac{\rho}{\Delta P}} = \frac{m}{\sqrt{\rho \cdot \Delta P}} \tag{9}$$

In design condition, this value can be determined for each valve. Considering the valve in design condition to be not completely open, an oversized CV for each valve can be defined ($CV_{max} = \alpha_v \cdot CV_{des}$). A typical operating range for each valve can thus be imposed:

$$CV_{low} = \alpha_{v,low} \cdot CV_{max} \tag{10}$$

$$CV_{up} = \alpha_{v,up} \cdot CV_{max} \tag{11}$$

In off-design conditions, the mass flow rate and pressure drop through each valve can be calculated and a valve flow coefficient determined, thus the valve position can be defined. The off-design flow coefficient must respect the operating range of the valve ($CV_{low} \leq CV_{off} \leq CV_{up}$), if these bounds are not respected a valve of different size (smaller or bigger) must be chosen.

3. Results

The analysis has been carried out varying ambient air temperature from −15 °C to +45 °C. As a consequence, three thermodynamic conditions are changing at the same time: the condenser refrigerant inlet air temperature and mass flow rate and temperature of the exhaust gas from the gas turbine.

Increasing ambient air temperature, gas turbine's output power and electrical efficiency decrease, together with a reduction of the exhaust hot gas mass flow rate and an increment in their temperature (Figure 3). When ambient air temperature is lower than −8 °C and greater than 32 °C, the exhaust mass flow rate decreases sharply. At +15 °C, the exhaust gas temperature trend slightly changes its slope.

The exhaust gas temperature value is, for all ambient temperature considered, greater than the oil limit temperature. Hence, the oil temperature at the outlet of the *HRB* is imposed to be equal to its limit temperature ($T_B = 380$ °C) in each off-design case, and the oil mass flow rate can be determined. The electrical power output shows a similar trend for each fluid considered (Figure 4), indicating the best performances for benzene and toluene independently from the ambient air temperature considered. The power output of the bottoming cycle decreases when air temperature increases, with a more significant power drop for higher temperatures. The curve is visibly steeper also for ambient temperatures lower than −8 °C. The power output is strongly affected by the hot gas mass flow rate (that shows a similar trend, as it can be seen in Figure 3), while the effects of the hot gas temperature are less evident since the maximum oil temperature is imposed to be equal to its limit.

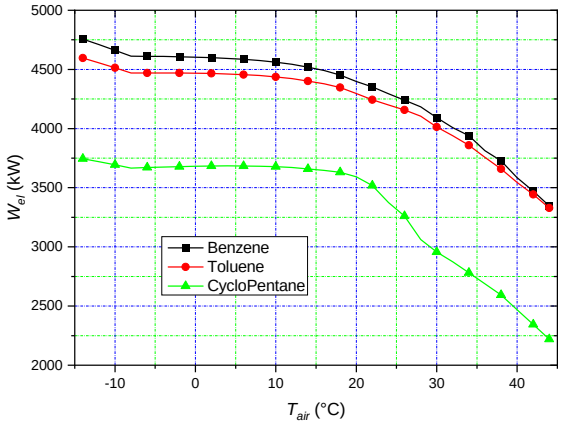

Figure 4. ORC electrical output power varying ambient temperature.

Considering Equation (4), each single contribution can be analysed. The power absorbed by the condenser fan (Figure 5) is not negligible; indeed, when ambient temperature increases, the control system, to maintain the pressure at the condenser constant, increases the air mass flow and, as a consequence, the pressure losses and power demand of the fan increase sharply (this can be clearly seen in Figure 5 for temperatures approaching 16 °C). When the air mass flow rate limit in the fan occurs (Figure 6), the control system imposes the maximum mass flow rate, resulting in an almost constant power absorption for temperatures above 16 °C (Figure 5), nonetheless a slight increase can still be appreciated, which is to be ascribed to the increase in the organic fluid pressure at the condenser. In the case of high ambient temperatures, an increase in the pressure at the condenser implies a higher saturation temperature for the organic fluid considered (Figure 1). The exhaust organic fluid temperature from the expander (T_2) tends to grow, as the expansion line is shorter. Consequently, the organic fluid temperature at the recuperator outlet (economizer inlet, T_6) is higher and the return oil temperature (T_E) increases as well.

A higher return oil temperature at *HRB* (T_A) reduces the heat exchanged with the hot gas stream inside the *HRB*, leading to an increase in the exhaust gas stack temperature (Figure 7) and maintaining it always above its lower limit. Figure 8 shows the diathermic oil mass flow rate varying with ambient air temperature. When air temperature is lower than −8 °C, the oil mass flow rate decreases, since the hot gas mass flow rate decreases as well (Figure 3). When ambient air temperature is between −8 °C and 16 °C, the oil mass flow rate is almost constant, for the reduction of hot mass flow rate is compensated by the gain in temperature of the hot gas stream (Figure 3). When ambient air

temperature rises above 16 °C, the return oil temperature increases and the oil mass flow rate increases again. Once the air temperature reaches 33 °C, the hot gas mass flow rate decreases sharply with respect to the increase in its temperature, leading to a decrease in the oil mass flow rate too.

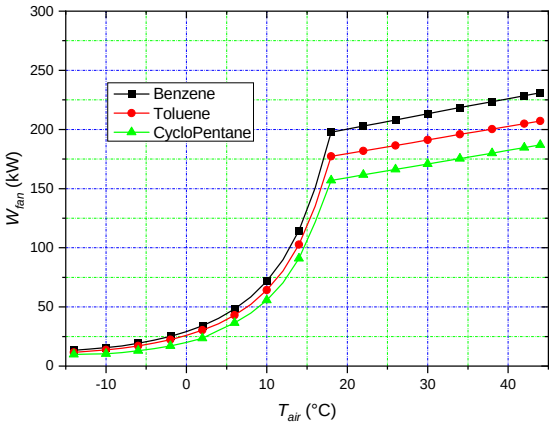

Figure 5. Power absorbed from condenser fan varying ambient temperature.

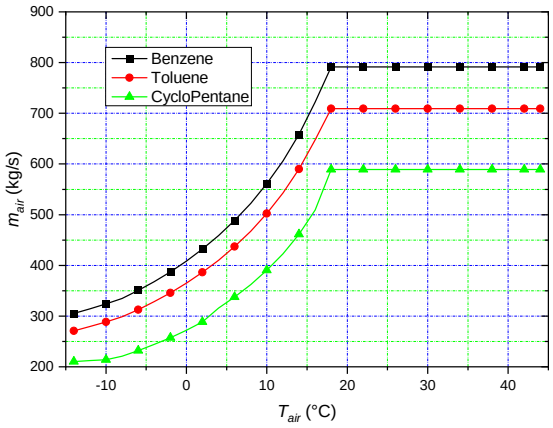

Figure 6. Condenser air mass flow rate varying ambient temperature.

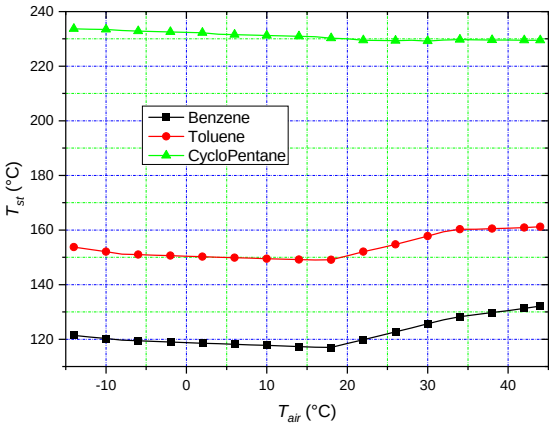

Figure 7. Stack temperature of exhaust gas varying ambient temperature.

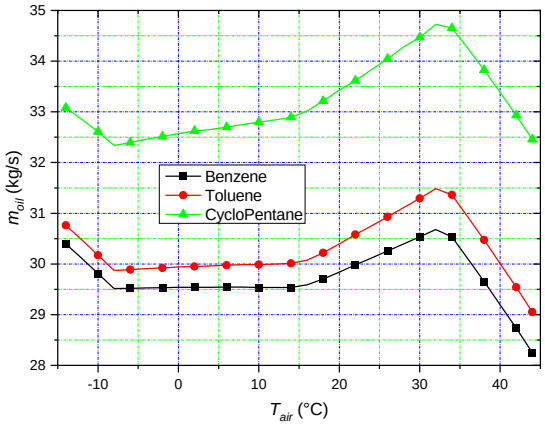

Figure 8. Diathermic oil mass flow rate varying ambient temperature.

Figure 9 shows the organic fluid mass flow rate as a function of ambient air temperature. The curves show a trend similar to those of the oil mass flow rates seen in Figure 8. Given the small magnitude of the subcooling inside the evaporator, from the energy balances it is possible to verify that the ratio between the fluid and oil mass flow rate is almost constant. The power absorbed from the organic fluid pump (Figure 10) presents quite the same trend of the organic fluid mass flow rate (Figure 9). The organic fluid mass flow rate variations are contained (lower than 8%), hence the expander inlet pressure oscillations are not relevant and show a trend similar to the fluid mass flow rate. Figure 11 presents the specific work per unit mass of the expander. It is almost constant for ambient air temperatures below 18°C; however, when the condenser's fan reaches its mass flow rate limit and the pressure at the condenser still increases, the specific work will start decreasing.

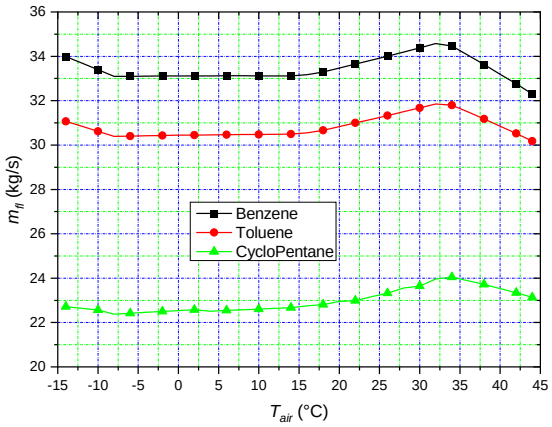

Figure 9. Organic fluid mass flow rate varying ambient temperature.

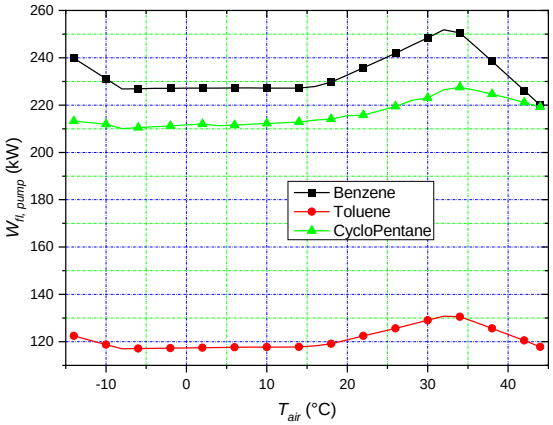

Figure 10. Power absorbed by organic fluid pump varying ambient temperature.

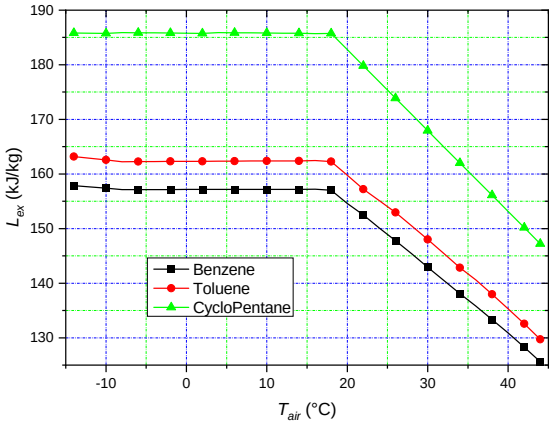

Figure 11. Expander specific work varying ambient temperature.

4. Conclusions

An Organic Rankine Cycle used as a bottoming cycle of a gas turbine has been investigated. An off-design performance analysis varying ambient air temperature (from −15 °C to 45 °C) with three different organic fluids has been performed; all three fluids have shown similar behaviours, however, benzene and toluene have proved to be more performing than cyclopentane. The benzene-based cycle power output varies between 4518 kW and 3346 kW in the ambient air temperature range considered.

The electric power output of the ORC decreases when ambient air temperature increases. This trend is mainly due to two distinct effects: the gas turbine exhaust mass flow rate decrease and the maximum air mass flow rate of condenser fan. The former effect could be partially counterbalanced by the increase in the hot gas temperature, yet it results ineffective in doing so, since the maximum oil temperature is reached and imposed to be constant. The latter effect brings an increase in fluid pressure at the condenser: the expander specific work decreases and the heat recovered in the *HRB* decreases accordingly. These considerations highlight the importance of a correct sizing of the condenser in design conditions, since it will affect the off-design behaviour of the entire cycle.

Future developments within this research topic could extend the study of the analysed power plant under off-design conditions using mixed working fluids, such as a benzene-toluene binary mixture, which can ensure better temperature glide so as to identify the most thermodynamically beneficial working fluids.

Author Contributions: Conceptualization, C.C. and L.W.; Data curation, L.W.; Formal analysis, L.C. and P.L.; Project administration, C.C.; Software, L.W.; Supervision, C.C.; Validation, L.C. and P.L.; Writing–original draft, L.W.; Writing–review and editing, L.C. and P.L. All authors have read and agreed to the published version of the manuscript.

Funding: This research received no external funding.

Conflicts of Interest: The authors declare no conflict of interest.

Abbreviations

The following abbreviations and nomenclature are used in this manuscript:

Greek

α	Valve CV corrective coefficient
η	effectiveness
ρ	density

Abbreviations

CON	Condenser
ECO	Economizer
EV	Evaporator
EX	Turbo-Expander
GWP	Global Warming Potential
HRB	Heat Recovery Boiler
HRSG	Heat Recovery Steam Generator
HTC	Heat Exchange Coefficient
ODP	Ozone Depletion Potential
ORC	Organic Rankine Cycle
REC	Recuperator
SICPL	Specific Investment Cost Part Load
SH	Superheater
TLV	Threshold Limit Value

Subscripts

air	external air
app	approach point
con	condenser
des	design
ex	exit
exh	exhaust
ext	external
fan	condenser fan
fl	organic fluid
int	internal
max	maximum
ml	logarithmic mean
oil	diathermic oil loop
off	off-design
pp	pinch point
$pump$	circuit pump
st	stack
sub	sub cooling
up	upper limit
v	valve

Symbol

A	Heat exchanger area
a	Reynolds exponent
C	Coefficient
CV	Valve discharge coefficient
f	Friction factor
k	Thermal conductivity
m	Mass flow rate
Nu	Nusselt number
Q	Heat output
R	Thermal resistance
Re	Reynolds number
s	Heat exchanger thickness
U	Global heat exchange coefficient
W	Power output

References

1. Hung, T.C.; Shai, T.; Wang, S.K. A review of organic Rankine cycles (ORCs) for the recovery of low-grade waste heat. *Energy* **1997**, *22*, 661–667.
2. Quoilin, S.; Orosz, M.; Hemond, H.; Lemort, V. Performance and design optimization of a low-cost solar organic Rankine cycle for remote power generation. *Sol. Energy* **2011**, *85*, 955–966.
3. Schuster, A.; Karellas, S.; Kakaras, E.; Spliethoff, H. Energetic and economic investigation of Organic Rankine Cycle applications. *Appl. Therm. Eng.* **2009**, *29*, 1809–1817.
4. Manente, G.; Toffolo, A.; Lazzaretto, A.; Paci, M. An Organic Rankine Cycle off-design model for the search of the optimal control strategy. *Energy* **2013**, *58*, 97–106, doi:10.1016/j.energy.2012.12.035.
5. Łukowicz, H.; Kochaniewicz, A. Analysis of the use of waste heat obtained from coal-fired units in Organic Rankine Cycles and for brown coal drying. *Energy* **2012**, *45*, 203–212.
6. Hung, T.; Wang, S.; Kuo, C.; Pei, B.; Tsai, K. A study of organic working fluids on system efficiency of an ORC using low-grade energy sources. *Energy* **2010**, *35*, 1403–1411.
7. Chen, H.; Goswami, D.Y.; Stefanakos, E.K. A review of thermodynamic cycles and working fluids for the conversion of low-grade heat. *Renew. Sustain. Energy Rev.* **2010**, *14*, 3059–3067.
8. Bhargava, R.K.; Bianchi, M.; Branchini, L.; De Pascale, A.; Orlandini, V. Organic rankine cycle system for effective energy recovery in offshore applications: A parametric investigation with different power rating gas turbines. In Proceedings of the ASME Turbo Expo 2015: Turbine Technical Conference and Exposition, Montreal, QC, Canada, 15–19 June 2015; p. V003T20A004.
9. Carcasci, C.; Ferraro, R. Thermodynamic Optimization and Off-Design Performance Analysis of a Toluene Based Rankine Cycle for Waste Heat Recovery from Medium-Sized Gas Turbines. In Proceedings of the ASME 2012 Gas Turbine India Conference, Mumbai, India, 1 December 2012; pp. 761–772.
10. Dai, Y.; Wang, J.; Gao, L. Parametric optimization and comparative study of organic Rankine cycle (ORC) for low grade waste heat recovery. *Energy Convers. Manag.* **2009**, *50*, 576–582.
11. Roy, J.; Mishra, M.; Misra, A. Parametric optimization and performance analysis of a waste heat recovery system using Organic Rankine Cycle. *Energy* **2010**, *35*, 5049–5062.
12. Wei, D.; Lu, X.; Lu, Z.; Gu, J. Performance analysis and optimization of organic Rankine cycle (ORC) for waste heat recovery. *Energy Convers. Manag.* **2007**, *48*, 1113–1119.
13. Guo, C.; Du, X.; Yang, L.; Yang, Y. Performance analysis of organic Rankine cycle based on location of heat transfer pinch point in evaporator. *Appl. Therm. Eng.* **2014**, *62*, 176–186.
14. Sun, J.; Li, W. Operation optimization of an organic Rankine cycle (ORC) heat recovery power plant. *Appl. Therm. Eng.* **2011**, *31*, 2032–2041.
15. Chen, Q.; Xu, J.; Chen, H. A new design method for Organic Rankine Cycles with constraint of inlet and outlet heat carrier fluid temperatures coupling with the heat source. *Appl. Energy* **2012**, *98*, 562–573.
16. Li, J.; Pei, G.; Li, Y.; Wang, D.; Ji, J. Energetic and exergetic investigation of an organic Rankine cycle at different heat source temperatures. *Energy* **2012**, *38*, 85–95.

17. Chacartegui, R.; Sánchez, D.; Muñoz, J.; Sánchez, T. Alternative ORC bottoming cycles for combined cycle power plants. *Appl. Energy* **2009**, *86*, 2162–2170.
18. Del Turco, P.; Asti, A.; Del Greco, A.S.; Bacci, A.; Landi, G.; Seghi, G. The ORegen^{TM} waste heat recovery cycle: Reducing the CO2 footprint by means of overall cycle efficiency improvement. In Proceedings of the ASME 2011 Turbo Expo: Turbine Technical Conference and Exposition, Vancouver, BC, Canada, 6–10 June 2011; pp. 547–556.
19. Carcasci, C.; Ferraro, R.; Miliotti, E. Thermodynamic analysis of an organic Rankine cycle for waste heat recovery from gas turbines. *Energy* **2014**, *65*, 91–100.
20. Gas Turbine World. *2016-2017 Gas Turbine World Handbook*, 1sted. Pequot Publishing Inc.: Fairfield, CT, USA, **2017**, 51
21. Quoilin, S.; Aumann, R.; Grill, A.; Schuster, A.; Lemort, V.; Spliethoff, H. Dynamic modeling and optimal control strategy of waste heat recovery Organic Rankine Cycles. *Appl. Energy* **2011**, *88*, 2183–2190.
22. Song, J.; Gu, C.W.; Ren, X. Parametric design and off-design analysis of organic Rankine cycle (ORC) system. *Energy Convers. Manag.* **2016**, *112*, 157–165, doi:10.1016/j.enconman.2015.12.085.
23. Cao, Y.; Dai, Y. Comparative analysis on off-design performance of a gas turbine and ORC combined cycle under different operation approaches. *Energy Convers. Manag.* **2017**, *135*, 84–100, doi:10.1016/j.enconman.2016.12.072.
24. Wei, D.; Lu, X.; Lu, Z.; Gu, J. Dynamic modeling and simulation of an Organic Rankine Cycle (ORC) system for waste heat recovery. *Appl. Therm. Eng.* **2008**, *28*, 1216–1224.
25. Sauret, E.; Gu, Y. Three-dimensional off-design numerical analysis of an organic Rankine cycle radial-inflow turbine. *Appl. Energy* **2014**, *135*, 202–211.
26. Fu, B.R.; Hsu, S.W.; Lee, Y.R.; Hsieh, J.C.; Chang, C.M.; Liu, C.H. Effect of off-design heat source temperature on heat transfer characteristics and system performance of a 250-kW organic Rankine cycle system. *Appl. Therm. Eng.* **2014**, *70*, 7–12.
27. Ibarra, M.; Rovira, A.; Alarcón-Padilla, D.C.; Blanco, J. Performance of a 5 kWe Organic Rankine Cycle at part-load operation. *Appl. Energy* **2014**, *120*, 147–158.
28. Bamgbopa, M.O.; Uzgoren, E. Numerical analysis of an organic Rankine cycle under steady and variable heat input. *Appl. Energy* **2013**, *107*, 219–228.
29. de Escalona, J.M.; Sánchez, D.; Chacartegui, R.; Sánchez, T. Part-load analysis of gas turbine & ORC combined cycles. *Appl. Therm. Eng.* **2012**, *36*, 63–72.
30. Lecompte, S.; Huisseune, H.; Van den Broek, M.; De Schampheleire, S.; De Paepe, M. Part load based thermo-economic optimization of the Organic Rankine Cycle (ORC) applied to a combined heat and power (CHP) system. *Appl. Energy* **2013**, *111*, 871–881.
31. Calise, F.; Capuozzo, C.; Carotenuto, A.; Vanoli, L. Thermoeconomic analysis and off-design performance of an organic Rankine cycle powered by medium-temperature heat sources. *Sol. Energy* **2014**, *103*, 595–609.
32. Quoilin, S.; Declaye, S.; Tchanche, B.F.; Lemort, V. Thermo-economic optimization of waste heat recovery Organic Rankine Cycles. *Appl. Therm. Eng.* **2011**, *31*, 2885–2893.
33. Carcasci, C.; Winchler, L. Thermodynamic analysis of an Organic Rankine Cycle for waste heat recovery from an aeroderivative intercooled gas turbine. *Energy Procedia* **2016**, *101*, 862–869.